Phase transformation during continuous heating in a β-quenched Ti-5Al-3Mo-3V-2Cr-2Zr-1Nb-1Fe alloy

Cong Wu[1,2*], Yongqing Zhao[2*], Qiaoyan Sun[1], Lian Zhou[2]

[1]*State Key Laboratory for Mechanical Behavior of Materials, Xi'an Jiaotong University, Xi'an 710049, China*

[2]*Northwest Institute for Non-ferrous Metal Research, Xi'an 710016, China*

E-mail addresses: cong_wu@163.com (Cong Wu), trc@c-nin.com(Yongqing Zhao).

Abstract

As a new near β titanium alloy designed by NIN (the Northwest Institute for Non-ferrous Metal Research), the phase transformations of the β-quenched Ti-5Al-3Mo-3V-2Cr-2Zr-1Nb-1Fe alloy during continuous heating have been investigated by means of in situ dilatometer test coupled with X-ray diffraction (XRD), scanning electron microscopy (SEM) and transmission electron microscopy (TEM). The β-quenched Ti-5321 alloy with an initial structure consisting of metastable β phase and dense ω_{ath}, which was subjected to continuous heating treatment and underwent the following transformations: $\beta + \omega_{ath} \rightarrow \beta + \omega_{iso} \rightarrow \beta + \alpha + \omega_{iso} \rightarrow \beta + \alpha$. The ω_{iso} phase precipitated at 300 ℃ with a ~3 nm ellipsoidal morphology. When continuously heated to 390 ℃, a coexistence of both ω_{iso} and α phase was observed in the β matrix, the platelet-like α phase closely nucleating at the ω/β interface with ~1 nm in width and ~8 nm in length. The α phase subsequently developed into lamellar structure when heated to higher temperatures, with a width of ~20 nm at 570 ℃ and ~85 nm at 690 ℃ respectively. Meanwhile, these α laths were uniformly distributed and composed of two distinct orientations within the microstructure. Finally, it can be found that the α morphology is directly associated with the formation and decomposition of the metastable ω_{iso} phase which may lead to the homogeneous and fine distribution of α precipitates. Based on the study of phase transformations occurring during the continuous heating process presented in this paper, an efficient guidance to engineer the microstructures and mechanical properties of this new near β titanium alloy was offered.

1. Introduction

Titanium alloys with high strength and toughness fill an important role in the aerospace industry, like Ti-10V-2Fe-3Al, Ti-3Al-8V-6Cr-4Zr-4Mo, Ti-5Al-5V-5Mo-3Cr-0.5Fe are known to be in steady production[1]. But the contradiction between strength and toughness has always been the challenge of these β titanium alloys, so new β titanium alloys need to be discovered and developed with high strength and toughness. For this reason, much efforts have focused on the development of titanium alloys with improved strength and toughness. For example, a new near titanium alloy Ti-7Mo-3Nb-3Cr-3Al was developed to get a combination of high strength and improved fracture toughness[2], Ti-1300 alloy as a near-β high strength titanium alloy can achieve an excellent combination of high strength and good ductility[3]. Recently, a new Ti-5Al-5Mo-3V-3Cr-2Zr-1Fe (Ti-5321) alloy, which has been developed in NIN (the Northwest Institute for Non-

ferrous Metal Research), with Fe and Nb are added simultaneously for the first time in the high strength titanium alloy design[4, 5].

As is known that the mechanical properties of β titanium alloys are strongly determined by the microstructure, in which the distribution and the size of α precipitates in the β matrix play an important role [6]. What's more, the α precipitates strongly influenced by the phase transformation pathways, the metastable phases like ω or β′. The subsequent aging heat treatments applied to β titanium alloys can trigger fine α phase precipitation in the β matrix, significantly increasing their mechanical strength[7, 8]. So it is essential to analyze the sequences and the resulting microstructures during heating process, in turn to engineer the α phase in near β titanium alloys and hence control mechanical properties.

It is known that ω phase result in drastic embrittlement, but when aged at proper temperatures, fine scale α phase precipitation in titanium alloys can leading to extremely high strength. Therefore, this metastable ω phase has intrigued researchers' interests for many years, on the one hand, its mechanism of formation is complex; on the other, it's a vital phase to tailor the multiphase microstructures of titanium alloys for various specific applications. According to the formation process, two forms of ω phase are distinguished, athermal ω (ω_{ath}) and isothermal ω (ω_{iso}). The ω_{ath} is commonly observed on rapidly cooling from the single β phase field, retaining the composition of the parent β matrix. The mechanism of ω_{ath} formation is diffusionless and displacive, the atomic shuffling, i.e. collapse of (111) β planes. While the ω_{iso} formed in subsequent isothermal aging, diffusion and displacive controlled, thus determined its irreversible nature. Owing to the characteristic of ω particles serving as heterogeneous nucleation sites for α precipitates. Several hypotheses have been proposed. According to the earlier literature reports[9], α phase tends to form some distance away from the β/ω interfaces. The ω-destabilizer element Al, usually rejected from ω phase. Some group concluded that, α phase nucleates inside ω phase by the diffusive and displacive mechanism[10]. More recently, lots of studies confirmed that α phase nucleates right at the β/ω interface. In the high misfit systems, the ω phase is cuboidal and α phase nucleates at ledges or dislocation on the β/ω interfaces. While in the low misfit system, the β/ω interfaces of ellipsoidal ω precipitates act as the nucleation sites due to the reduction of energy barrier for α nucleation[11-13].

Besides the ω phase, β′ phase, as a metastable phase, can also act as precursor for the precipitation of α phase. The β′ phase formed via the phase separation process, the β phase being rich with β stabilizing elements while the β′ phase being lean of β stabilizers. The mechanism of the consequent α phase precipitation on β′ phase has not been clearly defined. In the earlier research, the nucleation of α phase took place at the β′/β interface or within the β′ region[14]. The recent study proposed that α phase nucleates at the β/β′ interface and grows into the β′ phase by ledges[15]. Furthermore, the formation of a disordered orthorhombic O′ phase has been discovered in a fairly dilute binary Ti–Mo alloy, the O′ phase is transformed from the bcc lattice only by a {110}<1-10> shuffle[16].

As the metastable phase in the β titanium alloys are varied. Deep understanding of the phase transformations and microstructural modifications occurring during processing are thus required, which in turn allows the improvement of the mechanical performances. Recently, many researches focusing on the phase transformation mechanism in the β-quenched titanium alloy are carried out at this point. Usually the differential scanning calorimetry (DSC), in situ high energy synchrotron X-ray diffraction (HEXRD), electrical resistivity, ultrasonic measurement and the dilatometer test are performed[17-20]. Not only the transformation sequence, but the elemental partitioning and diffusion kinetics during the process are discussed thoroughly. Ti-5321, as a newly designed alloy, the phase transformation during continuous heating has not been studied yet as well as the correlation between the ω and α phase. Considering that the correlations between the

aging heat treatment conditions and microstructure of this new Ti-5321 alloys are not readily available, it is worth to investigate the phase transformation upon the presence of metastable ω phase.

In the present study, the phase transformations in the β-quenched Ti-5321 alloy during continuous heating have been investigated by means of in situ dilatometer test coupled with X-ray diffraction (XRD), scanning electron microscopy (SEM) and transmission electron microscopy (TEM). The phase transformation of ω phase and α phases were systematically analysed. This can offer a guidance to engineer the α phase in this new near β titanium alloys in the aging process and hence control mechanical properties. At the same time, the mechanism also available for other similar near β titanium alloys, such as Ti-5553 alloy and so on.

2. Experiment

2.1 Material

The as-received Ti-5321 alloy was hot-rolled at 830℃ without annealing. Table 1 shows the chemical composition of the alloy. The microstructure of the received alloy is shown in Fig. 1, corresponds to a transverse cut of the rod. Apparently, small globular primary α and fine lamellar/acicular uniformly are distributed within the β matrix.

Table 1 Chemical compositions of Ti-5321 alloy used in the present work (wt%)

Element	**Ti**	**Al**	**Mo**	**V**	**Cr**	**Zr**	**Nb**	**Fe**	**O**
wt.%	Bal.	5.02	3.03	2.99	2.06	2.01	1.37	0.99	0.064

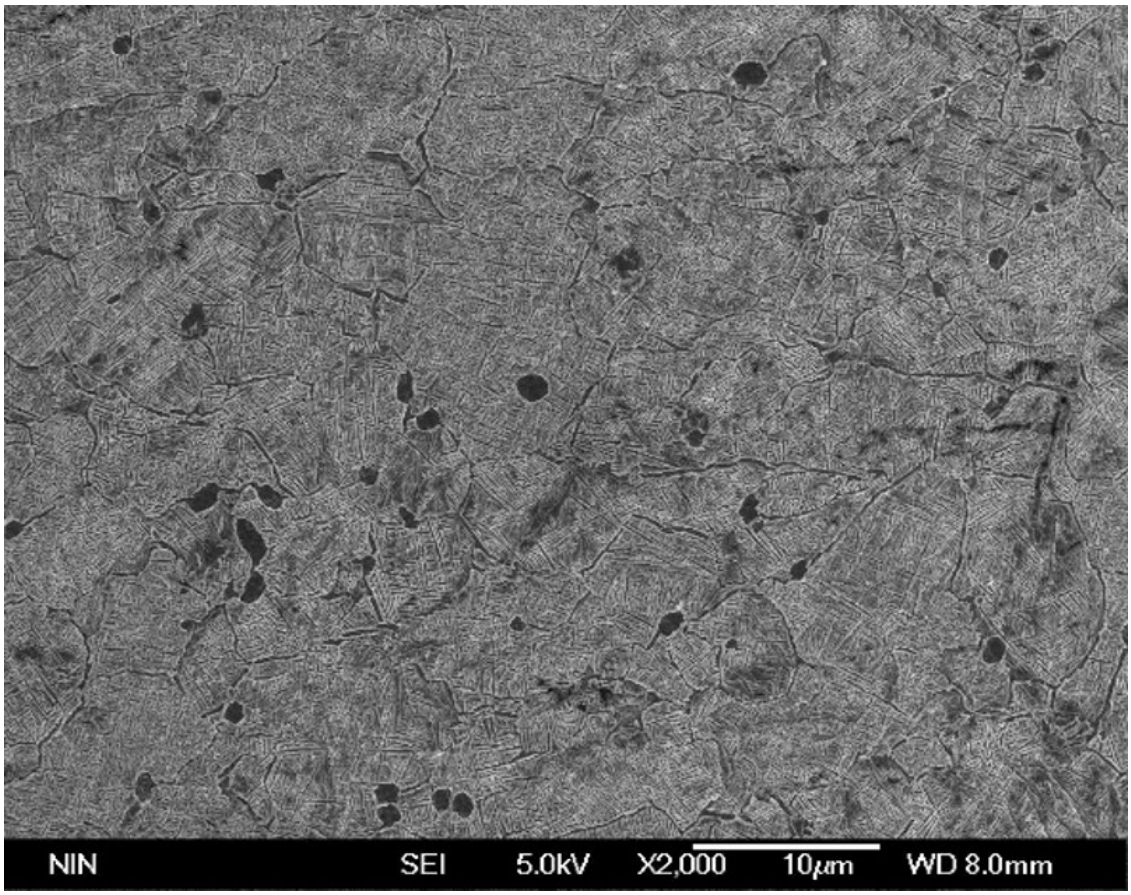

Fig. 1 Microstructure of Ti-5321 alloy after hot-rolled

2.2 Heat treatment

Based on the earlier research, the α/β transus temperature of Ti-5321 alloy is approximately 860℃. The sample cut from the received rod was solution-treated at 920 °C for 1 h, followed by water quenching (WQ). Subsequently, the dilatometric samples with a size of 5 mm in diameter and 10 mm in length cut from the solution-treated sample, then subjected to the continuous heating treatment at a heating rate of 0.1 ℃/s performed on the thermal dilatometer Bähr DIL805 A/D.

2.3 Microstructure characterization

Specimens for microstructure characterization were cut from the dilatometric samples perpendicular to the axis after the continuous heating treatment. A scanning electron microscopy (SEM) JSM-6700F and a transmission electron microscopy (TEM) JEM-2100 plus were used for microstructure observation and characterization. The specimens for SEM observation were ground, polished mechanically and then etched with Kroll solution (9% HF, 27% HNO_3 and 64% H_2O).

TEM samples thin foils were prepared via a twin-jet polishing method at the voltage of 35-45 V and the current of 30 mA in the mixed electrolyte of: perchloric acid (20 ml), methanol (200 ml), and n-butanol (400 ml).

3. Results and Discussion

3.1 Dilatometry analysis

The dilatometric (solid black) curve and its derivative (dotted red) curve of the β-quenched sample subjected to a continuous heating treatment at a heating rate of 0.1 ℃/s are shown in Fig. 2. The kinks on the dilatometric curve can be clearly seen in the derivative curve which are related to the phase transformations and marked as (a), (b), (c), (d). To confirm the phase transformations related to the kinks of dilatometric behaviors, another four β-quenched samples for the phase and microstructure observation were heated to 300 ℃, 390 ℃, 570 ℃ and 690 ℃ at a heating rate of 1 ℃/s respectively, followed by quenching at 80 ℃/s.

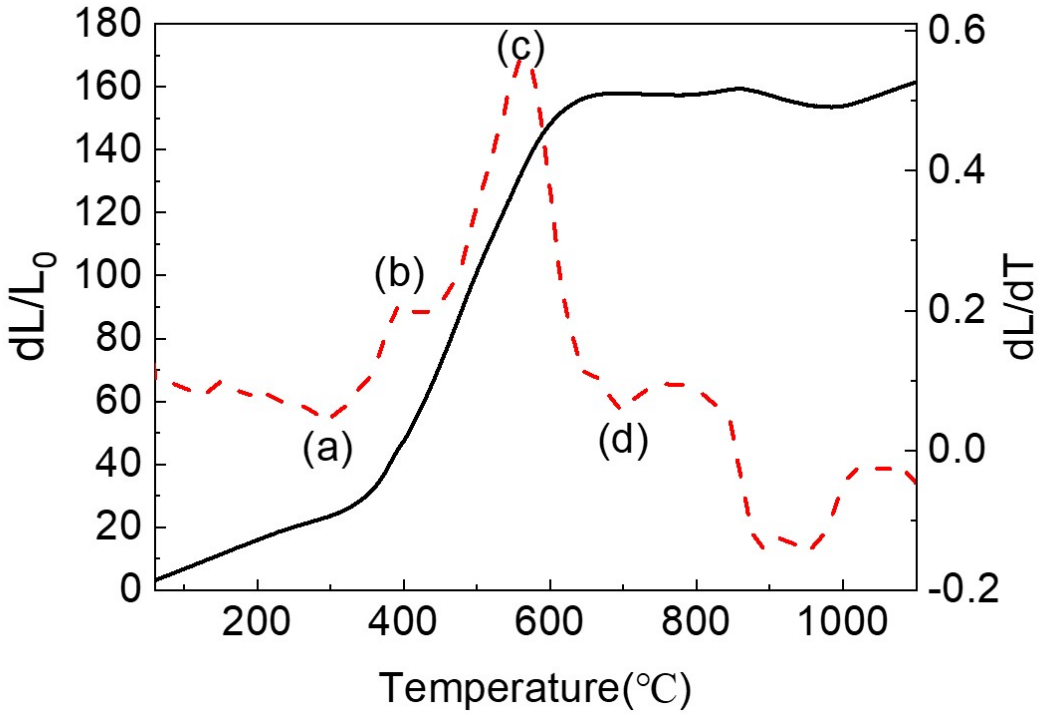

Fig.2 Dilatometric (solid) and derivative (dotted) curves of β-quenched Ti-5321 during continuous heating at 0.1 ℃/s

3.2 Microstructure analysis

As a near β alloy, Ti-5321 contains enough β-stabilizing elements to prevent the β-phase of decomposition upon quenching. In the bright-field image shown in Fig. 3a**,** the entire region corresponds to bcc β. The selected-area diffraction (SAD) pattern and dark field image show the existence of ω phase due to its nanoscale size, as shown in Fig. 3b and 3c. The SAD pattern along the [110] zone axis of bcc β phase shows clearly weak streaks, indicating the existence of the ω-related structure within the β phase. The weak streaks indicate the early stage of the formation of ordered ω phases, which is called the "lattice collapse" mechanism: two-thirds of the (111) planes in the β phase collapsing into the intermediate position leaving the adjacent (111) planes unaltered[21]. The corresponding dark-field images recorded from the faint streaks ω diffraction spots (marked by the circle in Fig. 3b) is shown in Fig. 3c. The homogeneously dispersion of nanoscale precipitates of the ω particles are relatively fine and have a large number density, which are usually named athermal ω phase (ω_{ath}). The ω_{ath} with an average size of <3 nm is formed by a diffusionless-displacive transformation upon quenching from the above β-transus temperature.

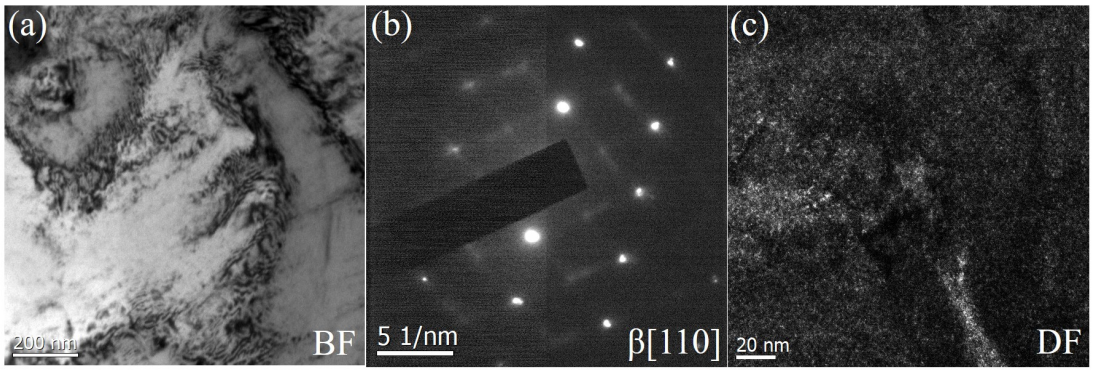

Fig.3 Microstructure of the β-quenched Ti-5321: (a) bright field image (BF) (b) SAD pattern along [110]β zone axis and (c) dark field image(DF)

Compared to the faint streaks in ω_{ath}, the diffraction spots at the 1/3 and 2/3 {112}β locations selected-area diffraction (SAD) patterns become substantially stronger and more pronounced when the temperature heating to 300℃, indicating the presence of ω_{iso} precipitates in this sample (as shown in Fig.4). In addition, two variants of ω are detected (ω_1 and ω_2) on this diffraction pattern. In dark image, ellipsoidal ω phase particles with a size of ~3 nm precipitate dispersed uniformly within the β matrix. What's more, the ellipsoidal shape of ω indicates that a low-misfit interface forms between ω and β inTi-5321 alloy.

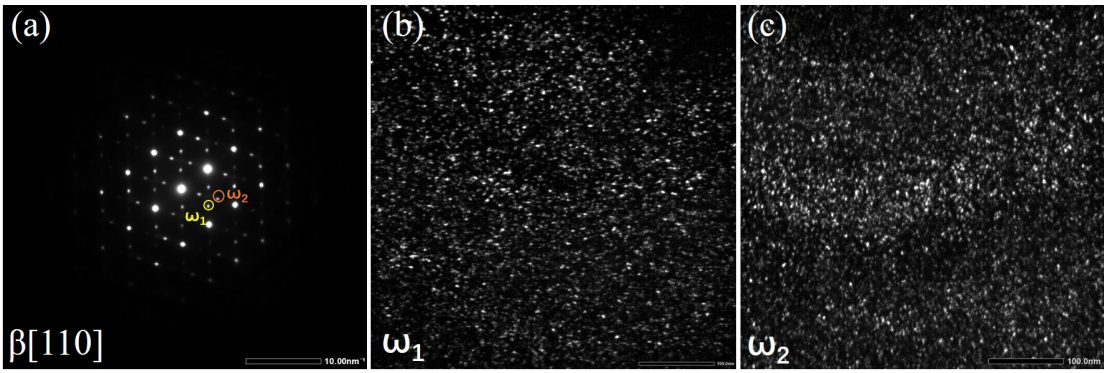

Fig.4 (a) the SAD patterns of the Ti-5321 heated up to 300 ℃ and the corresponding dark field image (DF) of (b) ω_1 and (c) ω_2

Fig. 5 shows the SAD pattern of the specimen which was heated to 390 ℃. An additional set of spots can be observed in comparison with the one presented in Fig. 4. These spots located at the middle of the four ω spots indicate the presence of the α-phase. Thus, a typical triple-phase microstructure of (ω+β+α) have been obtained at 390 ℃. As the HRTEM image clearly shown in Fig. 5c, two variants of ω phase are indicated along this zone axis, ellipsoidal in shape and ~6 nm in diameter, which is coarser than the ω phase in 300 ℃. The α phase exhibiting a plate shape with a size of ~8nm in length and ~1 nm thick near the β/ω interface which confirms that the α precipitation mechanism is "ω-assisted".

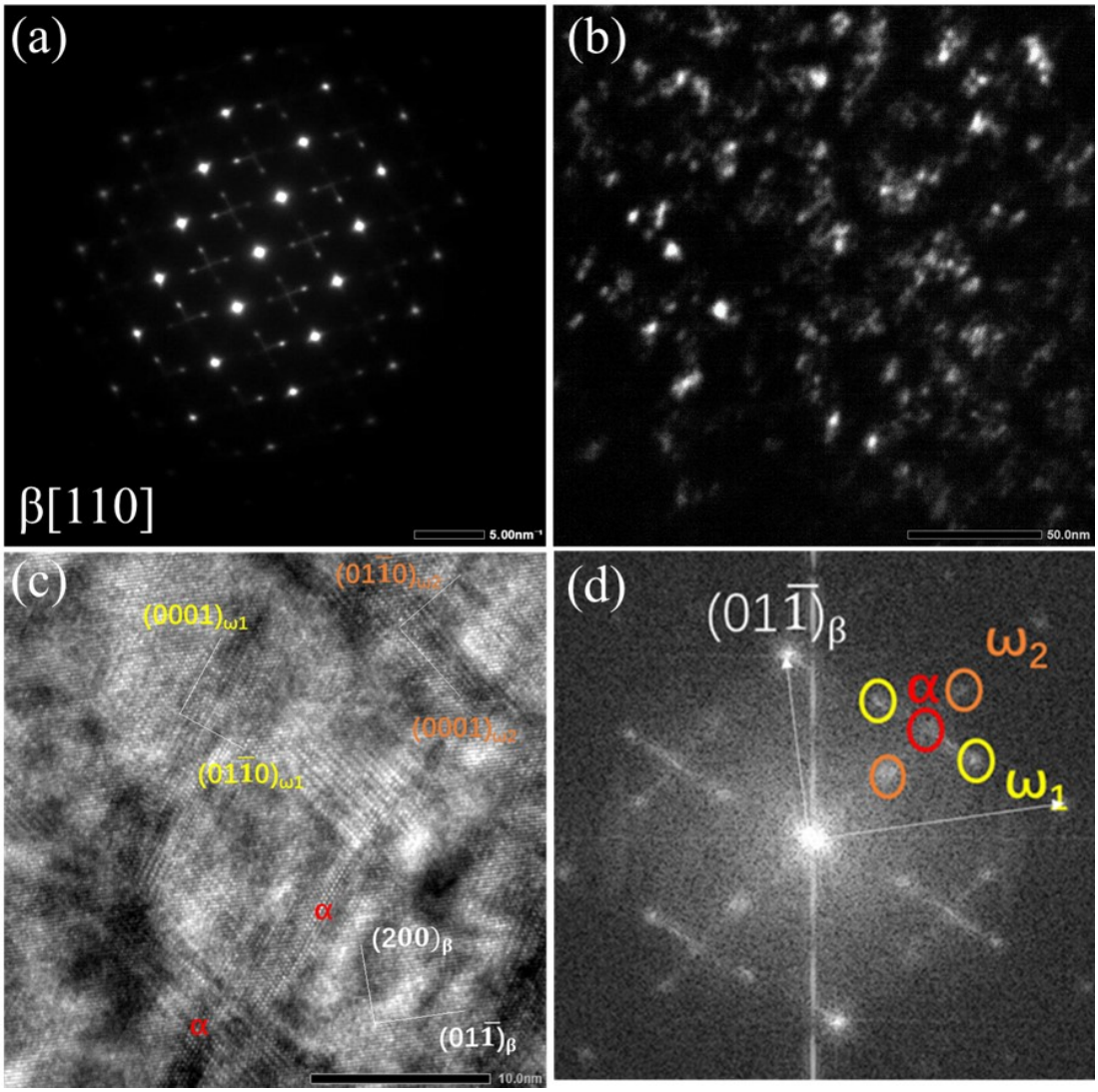

Fig. 5 (a) the SAD patterns of the Ti-5321 heated up to 390 ℃ and the corresponding dark field image (DF) of ω; (c) HRTEM image showing ω variants and β matrix with the [011]β zone axis and (d) the corresponding FFT diffractogram

The SEM and TEM images show that individual α precipitates develop into a chevron-like morphology when the temperature heating to 570 ℃, as shown in Fig. 6. The two arms of the chevrons with ~20 nm in width formed a dense microstructure. From the SAD pattern, only different α orientations spots can be found, the majority of ω_{iso} particles are demonstrated to revert back to β phase at this temperature. When the temperature increases to 690 ℃, the microstructure is

more like strings with a width of ~85 nm, as shown in Fig. 7. In fact, the α phase nucleates independently and then grows until mutual impingement occurs.

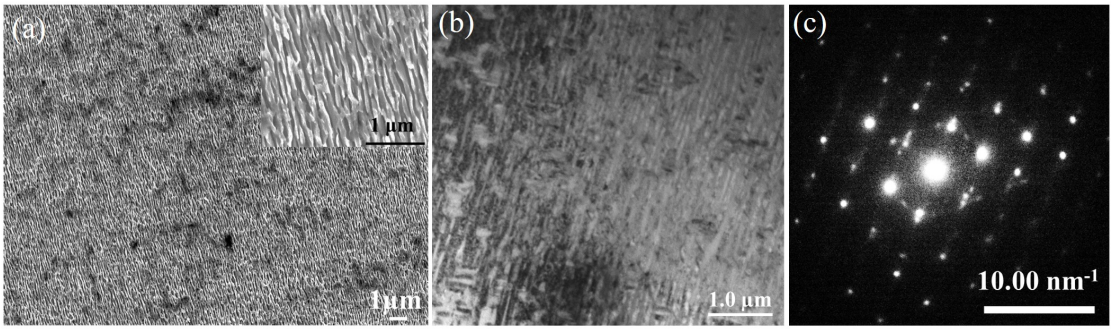

Fig. 6 The microstructure of Ti-5321 heated up to 570 ℃ (a) the SEM image (b) the TEM bright field image and (c) the SAD pattern

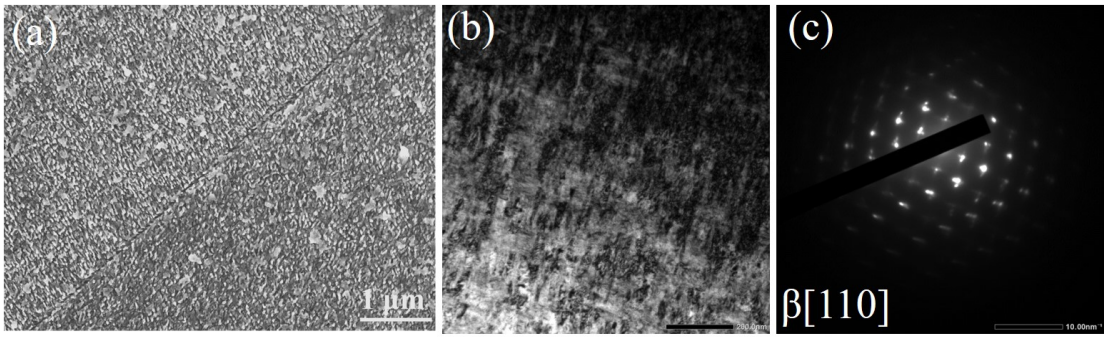

Fig. 7 The microstructure of Ti-5321 heated up to 690 ℃ (a) the SEM image (b) the TEM bright field image and and (c) the SAD pattern

4. Conclusion

The β-quenched Ti-5321 alloy with an initial structure consisting of metastable β phase and dense ω_{ath} was subjected to a continuous heating treatment. Four temperatures of 300 ℃, 390 ℃, 570 ℃ and 690 ℃ are chose to confirm the phase transformations and microstructure observation. Several obtained conclusions are as follows:

1. The phase transformation sequence is confirmed to be: $\beta + \omega_{ath} \rightarrow \beta + \omega_{iso} \rightarrow \beta + \alpha + \omega_{iso} \rightarrow \beta + \alpha$.
2. When the temperature was lower than 390 °C, the dimension of ω_{iso} phase would be expected to increase with temperature increasing. When the temperatures were higher than 570 °C, α precipitation should prevail with a chevron-like morphology, the width of α increase with temperature increasing.
3. The α phase transformation is supported to through a ω-assisted mechanism.

All of these discoveries and discussions provided a deeper understanding of the phase transformations in Ti-5321 alloy, as a guide for future evaluations of phase transformation in different temperatures and in other alloy systems.

Acknowledgements

This work was funded by the National Natural Science Foundation of China (Grants No. 51471136) and the National International Science and Technology Cooperation Project of China (Grants No. 2015DF151430).

References

[1] J. D. Cotton, R. D. Briggs, JOM 67(6) (2015) 1281-1303.

[2] J. Li, B. Tang, John Wiley & Sons, Inc.(2016) 869-872.

[3] J. W. Lu, Y. Q. Zhao, Mat. Sci. Eng. A 621 (2015) 182-189.

[4] Y. Zhao, C. Ma, Mater. China 35(12) (2016) 914-918.

[5] L. Ren, W. Xiao, Mat. Sci. Eng. A 711 (2017) 553-561.

[6] C. Huang, Y. Zhao, J. Alloys Compd. 693 (2017) 582-591.

[7] L. Ren, W. Xiao, Mater. Charact. 144 (2018) 553-561.

[8] C. R. M. Afonso, P. L. Ferrandini, Acta Biomaterialia 6(4) (2010) 1625-1629.

[9] S. Azimzadeh, H. J. Rack, Metall. Mater. Trans. A 29(10) (1998) 2455-2467.

[10] F. Prima, P. Vermaut, Scripta Mater. 54(4) (2006) 645-648.

[11] S. Nag, R. Banerjee, , Acta Mater. 57(7) (2009) 2136-2147.

[12] Y. Zheng, R. E. A. Williams, , Acta Mater. 103 (2016) 850-858.

[13] Y. Ohmori, T. Ogo, Mat. Sci. Eng. A 312(1–2) (2001) 182-188.

[14] J. C. Williams, B. S. Hickman, Metall. Trans. A 2(7) (1971) 1913-1919.

[15] Y. M. Zhu, S. M. Zhu, Scripta Mater. 112 (2016) 46-49.

[16] Y. Zheng, D. Banerjee, Scripta Mater. 116 (2016) 131-134.

[17] P. Barriobero-Vila, G. Requena, Acta Mater. 95 (2015) 90-101.

[18] F. Chen, G. Xu, Metall. Mater. Trans. A 47A(11) (2016) 5383-5394.

[19] A. Settefrati, M. Dehmas, Ti-2011. (2012) 468-472.

[20] J. Nejezchlebová, H. Seiner, J. Alloys Compd.762 (2018) 868-872.

[21] D. D. Fontaine, N. E. Paton, Acta Metall. 19(11) (1971) 1153-1162.